Self-motion of a phenanthroline disk on divalent metal ion aqueous solutions coupled with complex formation

Satoshi Nakata* and Yoshie Arima

Department of Chemistry, Nara University of Education, Takabatake-cho, Nara 630-8528, Japan

RECEIVED DATE

TITLE RUNNING HEAD: Self-motion of a phenanthroline disk

* Corresponding author. Tel: +81-742-27-9191; Fax: +81-742-27-9191; E-mail: nakatas@nara-edu.ac.jp.

Abstract

The self-motion of a 1,10-phenanthroline disk on divalent metal ion aqueous solutions was investigated as a simple autonomous motor coupled with complex formation. The characteristic features of motion (continuous and oscillatory motion) and their concentration regions differed among metal ions, and the frequency of oscillatory motion depended on the temperature of the aqueous solution. The nature of the characteristic motion is discussed in relation to the stability constant of complex formation between phenanthroline and a metal ion, and the difference in surface tension between phenanthroline and its metal complex as the driving force.

Keywords: self-motion, oscillation, nonequilibrium, air/water interface, driving force

1. Introduction

Various types of autonomous motors have been investigated at immiscible interfaces[1-19] not only to develop an inorganic miniature motor but also to better understand the mechanism of motion of microscopic organisms such as bacteria. These motors can move by obtaining driving force, which is induced by spatial anisotropy of their systems or by chemical nonequilibrium, e.g., a difference in the interfacial tension around a liquid droplet [4-9], bubble generation by the decomposition of H_2O_2 [10, 11], a spatial gradient in the hydrophobicity of a solid surface [12-16], application of an electronic field [17], and change in the volume of a gel [18, 19].

We have been studying the vector process and mode changes in fragments of camphor and its derivatives as a simple autonomous motor that can adapt to internal (mass, shape, and chemical structure of the mobile fragment) [20-23] and external (shape and size of the cell, and chemical property of the aqueous phase) conditions [24-26] under nonequilibrium and anisotropic environments. The essential features of this self-motion can be reproduced by a computer simulation based on the equation of motion coupled with reaction-diffusion equations and surface tension as the driving force [20-22, 24, 26].

We have recently reported the characteristic motion of a 1,10-phenanthroline disk on an aqueous phase with different concentrations of $FeSO_4$ as a complex-formation system [23]. However, the relationship between the kinetics of complex formation and motion has not yet been clarified. In this study, a 1,10-phenanthroline disk on divalent metal ion solutions was investigated with regard to complex formation. The concentration regions for characteristic motions (continuous and oscillatory motion) differed among these metal ions. The frequency of oscillatory motion increased with an increase in the temperature of the aqueous solution. The mechanism of these characteristic motions is discussed in relation to the surface tension on the 1,10-phenanthroline disk and the metal complex solution as the driving force, and the stability constant of the metal complex.

2. Experimental

All chemicals were analytical grade and used without further purification. Water was first distilled and then purified with a Millipore Milli-Q filtering system (pH of the obtained water: 6.3, resistance: > 20 MΩ). $FeSO_4$, $CoSO_4$, $MnSO_4$, $ZnSO_4$, $MgSO_4$, and $CaCl_2$ aqueous solutions were used as aqueous phases with divalent metal ions ($\mathbf{M}^{2+}$; **M**=Fe, Co, Mn, Zn, Mg, or Ca). A solid disk (diameter: 3 mm, thickness: 1 mm, mass: 7 mg) of 1,10-phenanthroline was prepared using a pellet die set. Twenty milliliters of the aqueous solution of different concentrations was poured into a glass Petri dish (inner diameter: 75 mm) as an aqueous phase (depth: 4.5 mm). The disk was carefully dropped on the aqueous phase from a few millimeter in height, and it floated from the start. Except for the experiments on temperature-dependence, the water cell was adjusted to 293 ± 1 K with a thermoplate (TP-80, AS ONE Co. Ltd., Japan). Movement of the disk was monitored with a digital video camera (SONY DCR-VX700, minimum time-resolution: 1/30 sec) and then analyzed by an image-processing system (Himawari, Library Inc., Japan). The surface tension at the air-water interface was measured with a surface tensiometer (CBVP-A3, Kyowa Interface Science Co., Ltd., Saitama, Japan), and a platinum plate (length, 23.85 mm; thickness, 0.15 mm) was used as the Wilhelmy plate. The speed of the motion (V) was obtained as $\sqrt{v_x^2 + v_y^2}$, where v_x and v_y were the velocities on the x- and y- directions, and the average speed (V_{av}) was obtained as the average value of V for 1 min after the disk was dropped on the aqueous phase except for collision with the Petri dish, and the reproducibility was examined for at least 4 times.

3. Results

Figure 1 shows (a) snapshots of the motion of a 1,10-phenanthroline disk on (1) 5 mM $FeSO_4$ and (2) 5 mM $MnSO_4$ aqueous solutions at 293 K, and (b) the time-variation of the speed in Fig.1a. With Fe^{2+} (Fig.1-1), oscillatory motion, i.e., repetition among rapid acceleration -> slow deceleration -> rest, was maintained for ca. 5 min. The amplitude and period of this oscillatory motion were 10.2 ± 1.7 mm s^{-1} and 8.7 ± 0.8 s, respectively. The density of a red-colored layer around the disk increased with time in

the resting state, and then the disk rapidly accelerated to move to another location. With Mn^{2+}, continuous motion at 10.0 ± 1.1 mm s^{-1} was maintained for ca. 3 min. It was actually difficult to observe the layer along the trajectory as seen in Figure 1, but the color of the solution became pale yellow after several trajectories. The shape of the disk was almost maintained for the duration of 3 min observation.

Figure 2 shows a phase diagram of the mode of 1,10-phenanthroline motion that depended on the concentrations of different aqueous solutions ($FeSO_4$, $CoSO_4$, $MnSO_4$, $ZnSO_4$, $MgSO_4$, $CaCl_2$). Here, repetition between rapid acceleration and slow deceleration and a constant speed motion were categorized by oscillatory motion (**O**) and continuous motion (**C**). If the concentration region of the oscillatory motion existed between continuous motion, **C** was further classified by a lower concentration region ($\mathbf{C}_l$) and a higher concentration region ($\mathbf{C}_h$). With an increase in the concentrations of Fe^{2+}, Co^{2+}, Mn^{2+}, and Zn^{2+}, continuous motion ($\mathbf{C}_l$) changed to oscillatory motion (**O**), and reverted to continuous motion ($\mathbf{C}_h$) with a further increase in the concentration. No oscillatory motion was observed for Ca^{2+} or Mg^{2+}. The lower boundary concentration between continuous and oscillatory motion was in the order $Fe^{2+} < Co^{2+} < Zn^{2+} < Mn^{2+}$, and the higher boundary concentration between oscillatory and continuous motion was in the order $Fe^{2+} < Co^{2+} < Zn^{2+}$, Mn^{2+} in the concentration regions examined.

Figure 3 shows (a) the surface tension depending on the concentration of a complex aqueous solution composed of tris-1,10-phenanthroline and a metal ion ($[Fe(phen)_3]^{2+}$ or $[Zn(phen)_3]^{2+}$), and (b) the average speed, v_{av}, depending on the concentration of $FeSO_4$ or $ZnSO_4$ aqueous solution. As seen for both Fe^{2+} and Zn^{2+} in Fig.3a, the surface tension of the complex solution, γ_c, decreased with an increase in concentration. The concentration regions of continuous ($\mathbf{C}_l$), oscillatory (**O**), and continuous motion ($\mathbf{C}_h$) for Fe^{2+} and Zn^{2+} almost corresponded to the concentrations at $\gamma_c > \gamma_p$, $\gamma_c \approx \gamma_p$, and $\gamma_c < \gamma_p$, respectively, where γ_p was the surface tension 5 mm from the edge of the 1,10-

phenanthroline disk which was fixed on water. Here, the distance, 5 mm, was selected based on the experimental results of the previous paper [27]. Here, γ_p decreased with time after the disk contacted water, and then reached a steady value after a few minutes. As seen in Fig.3b, v_{av} for Fe^{2+} and Zn^{2+} decreased with an increase in concentration up to the concentration regions of oscillatory motion. Above the concentration regions of oscillatory motion, v_{av} increased with an increase in concentration. The speed of continuous motion at the higher concentration region was more unstable than that at the lower concentration (see the error bar in Fig. 3b). A similar dependency was also observed for other metal ions (data not shown).

Next, the temperature of the aqueous phase was varied to clarify the relationship between complex formation and oscillatory motion. Figure 4 shows the time-variation of the speed of oscillatory motion for Fe^{2+} depending on the temperature of the aqueous phase. The resting state on the oscillatory motion was observed below 293 K (see Figures 4b and 1a-1). The period of oscillatory motion, τ_p, decreased with an increase in temperature, and a similar dependency was also observed for Co^{2+} (data not shown).

As for the influence of the shape of the disk, the intermittent oscillatory motion was independent of the shape of the disk since the resting time depended on the reaction time on the complex formation. In contrast, the nature of continuous motion depended on the shape of the disk [20, 24]. The speed of the motion was not very sensitive to the temperature of the aqueous phase under the present experimental conditions.

4. Discussion

Based on the experimental results and related papers on self-motion [20-26], we can discuss the mechanism of the characteristic motion of a phenanthroline disk depending on the kind of metal ion and the temperature. First, we consider the force around the disk on a metal ion solution, as indicated in Fig.5a. Here, we notice the horizontal force around the disk on a metal ion solution since the disk

moves on the aqueous phase. According to Young's force, the cross-section of the disk on the aqueous phase can be described as

$$f_d = (\gamma_R \sin\theta_R - \gamma_L \sin\theta_L)dx \quad (1)$$

where f_d is the driving force of the motion, γ_R and γ_L are the surface tension at the right and left points, θ_R and θ_L are the contact angles at the right and left sides, and dx is the length of the section of the disk.

If θ_R and θ_L are close to $\pi/2$ rad, eq.1 can be approximately rewritten as

$$f_d = (\gamma_R - \gamma_L)dx \quad (2)$$

The velocity of the motion, v, can be described as [20, 24]

$$m(dv/dt) = f_d - \mu v \quad (3)$$

where m is the mass of the disk and μ is the constant surface viscosity. If $dv/dt = 0$, i.e., the velocity reaches a constant value,

$$f_d = \mu v \quad (4)$$

Equations 2 and 4 suggest that the velocity of continuous motion is determined by the difference in the surface tension around the disk.

The direction of motion is thought to depend on the initial floating state of the disk [24]. Continuous motion on water without metal ions is due to the successive development of a phenanthroline layer, which plays an important role as the driving force (State I in Fig. 5) [23]. The decrease in speed with an increase in the concentration of the metal ions in the region of continuous motion at the lower concentration region ($\mathbf{C}_l$) is due to the decrease in surface tension as the driving force with an increase in the concentration of the metal complex which is formed around the disk, as seen in Fig. 3.

The mechanism of intermittent oscillatory motion may be explained as follows. When the disk rests or moves with a low speed on water, insoluble phenanthroline molecules, which develop from the solid disk to the water surface, immediately form a soluble complex (3phen + $\mathbf{M}^{2+} \rightarrow \mathbf{M}(\mathrm{phen})_3^{2+}$, **M**=Fe, Co, Mn, or Zn) around the disk (State IIα in Fig. 5). Thus, the driving force can not be obtained until there is a shortage of metal ions around the disk due to complex formation. The phenanthroline molecular layer as the driving force can then develop on the water surface when there is a shortage of metal ions (State IIβ in Fig. 5). Rapid acceleration suggests the existence of switching from complex formation to the development of a phenanthroline layer (see Fig. 1-1). As the phenanthroline disk moves to another location that has sufficient metal ions, motion decreases again. Thus, oscillatory motion is generated by the repetition of States IIα and β. We have reported that the period of oscillatory motion increases with an increase in the concentration of metal ions since the duration of the resting state corresponds to that of complex formation [23].

Above the concentration region for oscillatory motion, the driving force for continuous motion ($\mathbf{C}_h$) may switch to the surface tension of a metal complex layer produced around the phenanthroline disk (State III in Fig. 5), since the surface tension of a metal complex solution is lower than that of a

phenanthroline layer (69 mN m^{-1}) and the increase in speed with an increase in the concentration of metal complex corresponds to the further decrease in surface tension, as shown in Fig. 3 [28]. In addition, the solubility of the developed metal complex molecules in the aqueous phase decreases due to the existence of metal ions with a high concentration, and therefore the metal complex molecules tend to concentrate on the aqueous surface [23].

The stability constants, log K_3, for Fe^{2+}, Co^{2+}, Zn^{2+}, and Mn^{2+} are 21.3, 19.9, 17.6, and 10.1, respectively [29], where $K_3=[\mathbf{M}(phen)_3^{2+}]/[\mathbf{M}^{2+}][phen]^3$. The stability constants, log K_1, for Fe^{2+}, Co^{2+}, Zn^{2+}, Mn^{2+}, Mg^{2+} and Ca^{2+} are 5.85, 7.25, 6.55, 3.88, 1.2 and 0.7, where $K_1=[\mathbf{M}(phen)^{2+}]/[\mathbf{M}^{2+}][phen]$ [29]. The lack of oscillatory motion for Ca^{2+} and Mg^{2+}, which have low stability constants, and the decrease in the concentration region of oscillatory motion with an increase in K_3 for Fe^{2+}, Co^{2+}, Zn^{2+}, and Mn^{2+} suggest that complex formation plays an important role in oscillatory motion, as indicated in Fig. 2.

The relationship between the enthalpy, ΔH^o, and the equilibrium constant, K_3 (= k_c/k_{-c}) on the reaction of eq.5 can be expressed as

$$\ln K_3 = -\Delta H^o/RT + \Delta S^o/R \tag{5}$$

where R is the gas constant, ΔS^o is the entropy, and T (K) is the temperature.

The reaction kinetics for the formation of a complex composed of tris-(1,10-phenanthroline) and a metal ion around the water surface may be expressed as

$$dC_p/dt = S_0(C_0 - C_p) - k_c C_p^3 (C_{M0} - C_c) + 3k_{-c} C_c \tag{6}$$

$$dC_c/dt = k_c C_p^3 (C_{M0} - C_c) - k_{-c} C_c \tag{7}$$

where S_0 is the rate constant on the development of phenanthroline molecules developed from is solid, C_p is the surface concentration of phenanthroline, C_c is the concentration of a metal complex, C_{M0} is the initial concentration of a metal ion, C_0 is the maximum surface concentration of phenanthroline, $C_{M0} - C_c$ is the concentration of a metal ion, k_c is the rate constant of the forward reaction in complex formation, and k_{-c} is the rate constant of the backward reaction in complex formation.

Based on the above mechanism of oscillatory motion, C_p plays an important role in the driving force, i.e., the difference in the surface tension as the driving force is obtained when C_p is larger than the critical concentration, C_{cr}. Figure 6 shows the numerical simulation on the relationship between K_3 and τ based on eqs.6 and 7. Here, τ is the elapsed time until C_p is larger than C_{cr}. τ increases with an increase in K_3 since the complex formation reduces C_p in eq.6. In the present parameter region, τ may be approximately proportional to K_3 in the present parameter region, as seen in Fig.6b.

Since the stability constant, log K_n (n=1, 2, or 3), for complex formation between 1,10-phenanthroline and a metal ion (Fe^{2+}, Co^{2+}, Zn^{2+}, or Mn^{2+}) is considerably larger than 1, the forward reaction, i.e., complex formation, is preferred in eq.7. As seen in Fig. 4, the period of oscillatory motion, τ_p, is almost determined by the sum of the resting time and/or deceleration time of disk motion. In other words, the acceleration time, which corresponds to no reaction time, is very short. Thus, τ_p corresponds to the reaction time in complex formation, i.e., τ_p is long if K_3 is large, and vice versa. Thus, eq.5 can be rewritten as eq.8 if τ_p is proportional to K_3, as indicated in Figure 6:

$$\ln \tau_p \propto -\Delta H^o/RT \tag{8}$$

Figure 7 shows the dependence of the period of oscillatory motion, τ_p (s), on the temperature of the aqueous phase, T (K), based on eq.5. ln τ_p linearly depends on T^{-1} except for Fe^{2+} at T=313 K.

ΔH^o for Fe^{2+} and Co^{2+} on the oscillation are estimated to be –58 and –30 kJ mol^{-1} based on the slope of the approximated line. ΔH for Fe^{2+} and Co^{2+} were reported as –138.1 and –99.6 kJ mol^{-1} on the reaction of the complex formation [30]. Although these values obtained from Figure 7 are smaller than those in the reference 30, the relative relationship between Fe^{2+} and Co^{2+} is similar to one another.

5. Conclusion

The mode of self-motion of a phenanthroline disk was discussed in relation to the development of a phenanthroline layer or a complex layer around the disk, which changed the surface tension and played a role in the driving force of motion. The concentration regions and period of oscillatory motion were also discussed in relation to the stability product and kinetics of complex formation around the disk. Although we notice the kinetics of complex formation between phenanthroline and different metal ions in this study, diffusion and convection terms should be considered to clarify the mechanism in the future work. We have reported the influence of diffusion and convection [22, 24, 31].

According to the Curie-Prigogine theorem, scalar variables cannot couple with vector values under isotropic and linear nonequilibium conditions [32, 33]. This suggests that the introduction of anisotropic and nonequilibrium conditions can induce a controllable vectorial process in a reaction field [33]. Therefore, various features of movement can be designed coupled with reaction-diffusion kinetics under anisotropic and nonequilibrium conditions.

Our results suggest that various types of autonomous systems can be designed based on the relationship between the surface concentration and surface tension of the surface active substance as the driving force, and on coupling with a chemical reaction (e.g., redox reaction in the present paper) depending on the chemical structure. Although the periodicity at the lower temperature was irregular, as seen in Fig. 4b, the irregularity in the present system has not yet been confirmed to be deterministic chaos or quasiperiodicity, since the direction of the motion was random due to the symmetric disk and therefore the influence of the distribution of complex molecules on the self-motion could not be controlled. Although we have not yet developed a mathematical model for the change in the mode of

motion of a 1,10-phenanthroline disk coupled with complex formation, we have considered a model similar to that for the motion of a camphoric acid boat coupled with a neutral reaction [22].

Acknowledgment.

We thank Ms. Junko Kirisaka (Miharadai Junior High School, Osaka, Japan) for her technical assistance. This study was supported in part by a Grant-in-Aid for Scientific Research (No. 18550126) to S. N and the Asahi Glass Foundation.

References

[1] F. Brochard, D. Quere, P. G. de Gennes, Capillarity and Wetting Phenomenon: Drops, Bubbles, Pearls, Waves, Springer-Verlag, 2003.

[2] H. Linde, P. Schwartz, H. Wilke, in: T. S. Sϕrensen (Ed.), Dynamics and Instability of Fluid Interfaces, Springer-Verlag, Berlin, 1979.

[3] V. G. Levich, in: D. B. Spalding (Ed.), Physicochemical Hydrodynamics, Advance Publications Limited, London, 1977.

[4] C. D. Bain, G. D. Burnett-Hall, R. R. Montgomerie, Rapid motion of liquid drops, Nature, 372 (1994) 414-415.

[5] T. Yamaguchi, T. Shinbo, A novel interfacial engine between two immiscible liquids, Chem. Lett., 18 (1989) 935-938.

[6] F. D. Dos Santos, T. Ondarçuhu, Free-running droplets, Phys. Rev. Lett., 75 (1995) 2972-2975.

[7] N. Magome, K. Yoshikawa, Nonlinear Oscillation and Ameba-like Motion in an Oil/Water System, J. Phys. Chem., 100 (1996) 19102-19105.

[8] Y. Sumino, N. Magome, T. Hamada, K. Yoshikawa, Self-running droplet: Emergence of regular motion from nonequilibrium noise, Phys. Rev. Lett., 94 (2005) 068301-1-068301-4.

[9] K. Nagai, Y. Sumino, H. Kitahata, K. Yoshikawa, Mode selection in the spontaneous motion of an alcohol droplet, Phys. Rev. E, 71 (2005) 065301-1-065301-4.

[10] R. F. Ismagilov, A. Schwartz, N. Bowden, G. M. Whitesides, Autonomous movement and self-assembly, Angew. Chem. Int. Ed., 41 (2002) 652-654.

[11] Y. Wang, R. M. Hernandez, D. J. Barlett, J. M. Bingham, T. R. Kline, A. Sen, T. E. Mallouk, Bipolar electrochemical mechanism for the propulsion of catalytic nanomotors in hydrogen peroxide solutions, Langmuir, 22 (2006) 10451-10456.

[12] P. G. de Gennes, The dynamics of reactive wetting on solid surfaces, Physica A, 249 (1998) 196-205.

[13] É. Lorenceau, D. Quéré, Drops on a conical wire, J. Fluid Mech., 510 (2004) 29-45.

[14] F. Brochard, Motions of droplets on solid surfaces induced by chemical or thermal gradients, Langmuir, 5 (1989) 432-438.

[15] M. K. Chaudhury, G. M. Whitesides, How to make water run uphill, Science, 256 (1992) 1539-1541.

[16] K. Ichimura, S. –K. Oh, M. Nakagawa, Light-driven motion of liquids on a photoresponsive surface, Science, 288 (2000) 1624-1626.

[17] O. D. Velev, B. G. Prevo, K. H. Bhatt, On-chip manipulation of free droplets, Nature, 426 (2003) 515-516.

[18] Y. Hara, R. Yoshida, Self-oscillation of polymer chains induced by the Belousov-Zhabotinsky reaction under acid-free conditions, J. Phys. Chem. B, 109 (2005) 9451-9454.

[19] R. Yoshida, Y. Uesusuki, Biomimetic gel exhibiting self-beating motion in ATP solution, Biomacromolecules, 6 (2005) 2923-2926.

[20] S. Nakata, Y. Iguchi, S. Ose, M. Kuboyama, T. Ishii, K. Yoshikawa, Self-rotation of a camphor scraping on water: New insight into the old problem, Langmuir, 13 (1997) 4454-4458.

[21] Y. Hayashima, M. Nagayama, S. Nakata, A camphor grain oscillates while breaking symmetry, J. Phys. Chem. B, 105 (2001) 5353-5357.

[22] Y. Hayashima, M. Nagayama, Y. Doi, S. Nakata, M. Kimura, M. Iida, Self-motion of a camphoric acid boat sensitive to the chemical environment, Phys. Chem. Chem. Phys., 4 (2002) 1386-1392.

[23] S. Nakata, S. Hiromatsu, H. Kitahata, Multiple autonomous motions synchronized with complex formation, J. Phys. Chem. B, 107 (2003) 10557-10559.

[24] M. Nagayama, S. Nakata, Y. Doi, Y. Hayashima, A theoretical and experimental study on the unidirectional motion of a camphor disk, Phys. D, 194 (2004) 151-165.

[25] S. Nakata, J. Kirisaka, Y. Arima, T. Ishii, Self-motion of a camphanic acid disk on water with different types of surfactants, J. Phys. Chem. B, 110 (2006) 21131-21134.

[26] S. Nakata, Y. Doi, H. Kitahata, Synchronized sailing of two camphor boats in polygonal chambers, J. Phys. Chem. B, 109 (2005) 1798-1802.

[27] S. Nakata, Y. Hayashima, Spontaneous dancing of a camphor scraping, J. Chem. Soc., Faraday Trans., 94 (1998) 3655-3658

[28] K. Yoshikawa, T. Kusumi, M. Ukitsu, S. Nakata, Generation of periodic force with oscillating chemical reaction, Chem. Phys. Lett., 211 (1993) 211-213.

[29] R. C. Weast, M. J. Astle, W. H. Beyer, CRC Handbook of Chemistry and Physics, A Ready-Reference Book of Chemical and Physical Data, CRC Press: Boca Raton, Fla., 1967.

[30] G. Anderegg, Pyridinderivate als complexbildner VI. Reaktionsenthalpie und -entropie bei der bildung der metallkomplexe von 1,10-phenanthrolin und α,α'-dipyridyl, Helv. Chim. Acta, 46 (1963) 2813-2822.

[31] H. Kitahata, S. Hiromatsu, Y. Doi, S. Nakata, M. R. Islam, Self-motion of a camphor disk coupled with convection, Phys. Chem. Chem. Phys., 6 (2004) 2409-2414.

[32] I. Prigogine, Introduction to Thermodynamics of Irreversible Processes, John Wiley & Sons, New York, 1961.

[33] N. Boccara, Symmetries and Broken Symmetries in Condensed Matter Physics, IDSET, Paris, 1981.

Figure captions

Figure 1. (a) Snapshots of the motion (top view) and (b) time-variation of the speed of a 1,10-phenanthroline disk on (1) $FeSO_4$ and (2) $MnSO_4$ aqueous solutions at 5 mM. Time intervals in (a) were 0.5 s for 1-6, 7-13 in (1) and 1-15 in (2), and 7.1 s between 6 and 7 in (1). The horizontal bars in (b-1) and (b-2) correspond to the data in (a-1) and (a-2), respectively. The resting times for 1 and 13 in the intermittent motion in (a-1) were 3 sec.

Figure 2. Phase diagram of the mode of motion of a 1,10-phenanthroline disk depending on the concentration (C) of divalent metal ions aqueous solutions ($FeSO_4$, $CoSO_4$, $ZnSO_4$, $MnSO_4$, $CaCl_2$, and $MgSO_4$). $\mathbf{C_l}$, **O**, and $\mathbf{C_h}$ denote continuous motion at the lower concentration region, oscillatory motion, and continuous motion at the higher concentration region, respectively. The thickness of the gray lines corresponds to the regions of ambiguity at the boundaries between $\mathbf{C_l}$ and **O**, and between **O** and $\mathbf{C_h}$. For $CaCl_2$ and $MgSO_4$, the continuous motion is denoted as **C** since no oscillatory motion was observed.

Figure 3. (a) Surface tension depending on the concentration of tris-1,10-phenanthroline and Fe^{2+} complex ($[Fe(phen)_3]^{2+}$, filled circle), and tris-1,10-phenanthroline and Zn^{2+} complex ($[Zn(phen)_3]^{2+}$, empty circle) aqueous solutions. The dotted line denotes the surface tension (γ_p) when the minimum distance between the platinum blade to measure the surface tension and a 1,10-phenanthroline disk in contact with water was 5 mm. (b) The average speed of motion depending on the concentration of $FeSO_4$ (filled circle) and $ZnSO_4$ (empty circle) aqueous solutions. The dotted gray lines denote the concentration regions of oscillatory motion for Fe^{2+} and Zn^{2+}, which correspond to those in Fig. 2.

Figure 4. Time-variation of the speed of a 1,10-phenanthroline disk on a 5 mM $FeSO_4$ aqueous solution at (a) 303 and (b) 283 K.

Figure 5. Schematic representation of the mechanism of phenanthroline disk motion. (a) Forces around a 1,10-phenanthroline disk on an aqueous phase. γ_{as} is the interfacial tension at the air/solid interface and γ_{sl} is the interfacial tension at the solid/liquid interface. (b) States I, II, and III correspond to continuous motion at the lower concentration region ($\mathbf{C_l}$), oscillatory motion (**O**), and continuous motion at the higher concentration region ($\mathbf{C_h}$), respectively. States IIα and IIβ correspond to deceleration or rest without a driving force and motion driven by the surface tension, respectively.

Figure 6. Numerical calculation based on eqs.6 and 7. (a) Time variation of C_p at $K_3= 2\times10^4$ (dotted line), $K_3= 5 \times 10^4$ (solid line), and $K_3= 8 \times 10^4$ (thick solid line). $C_c = 0$ at $t=0$. τ is the time at the intersection between the curve of C_p and C_{cr} (gray dotted line). (b) Relationship between K_3 and τ. $S_0=C_{M0}=C_0=1$. $k_{-c}=1.0\times10^{-5}$, $C_{cr}=0.8$.

Figure 7. Logarithm of the period of oscillatory motion, $-\ln \tau_p$ (s), *versus* temperature (expressed as T^{-1} x 1000 (K^{-1})) for a 1,10-phenanthroline disk on 5 mM $FeSO_4$ (filled circle) and 10 mM $CoSO_4$ aqueous solutions. The data correspond to those in Fig. 4.

Figure 1

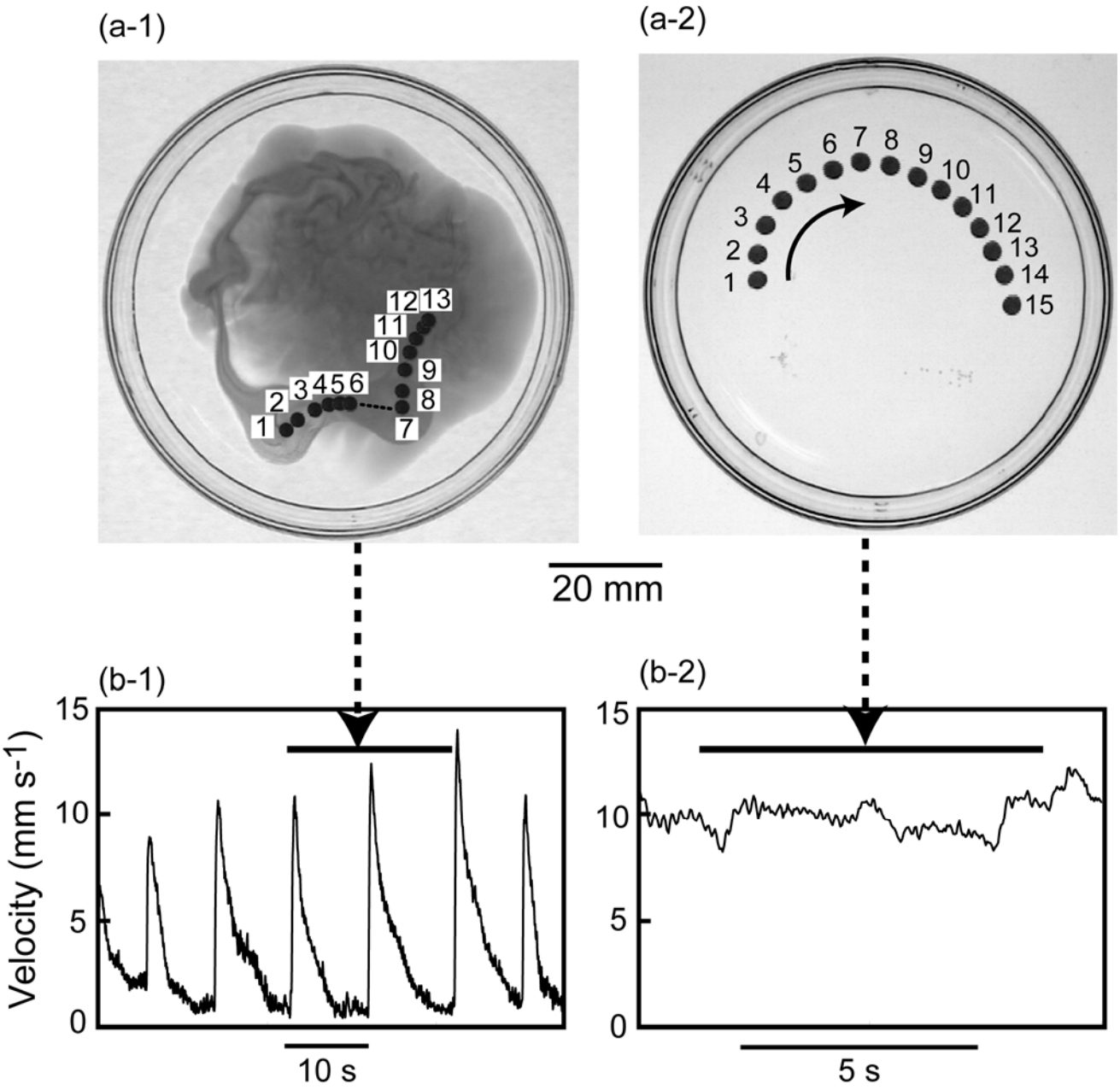
(a-1)
(a-2)
1
2
3
4
5
6
7
8
9
10
11
12
13
14
15
20 mm
(b-1)
(b-2)
Velocity (mm s-1)
15
10
5
0
10 s
5 s

Figure 2

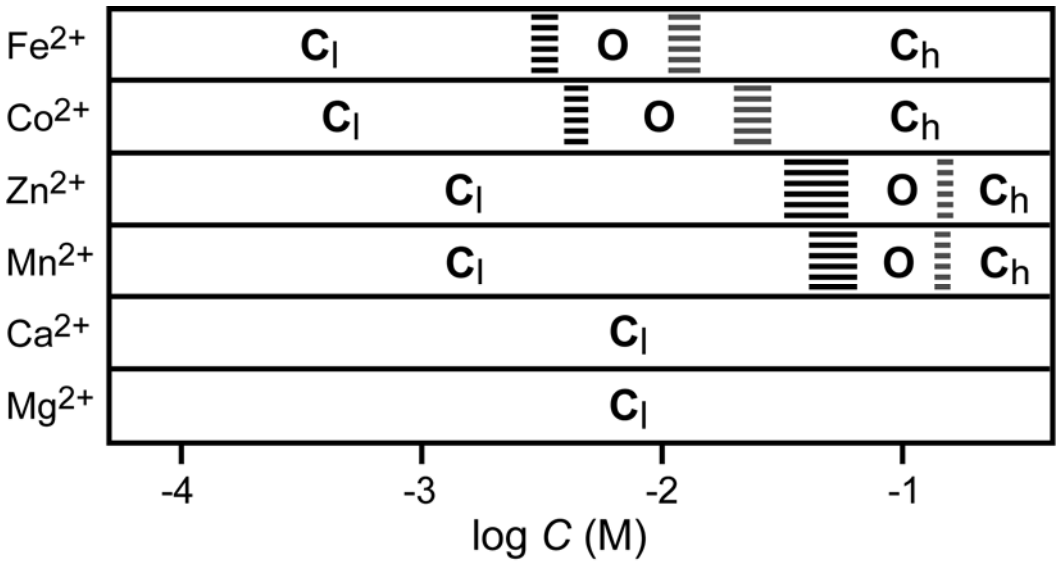

Figure 3

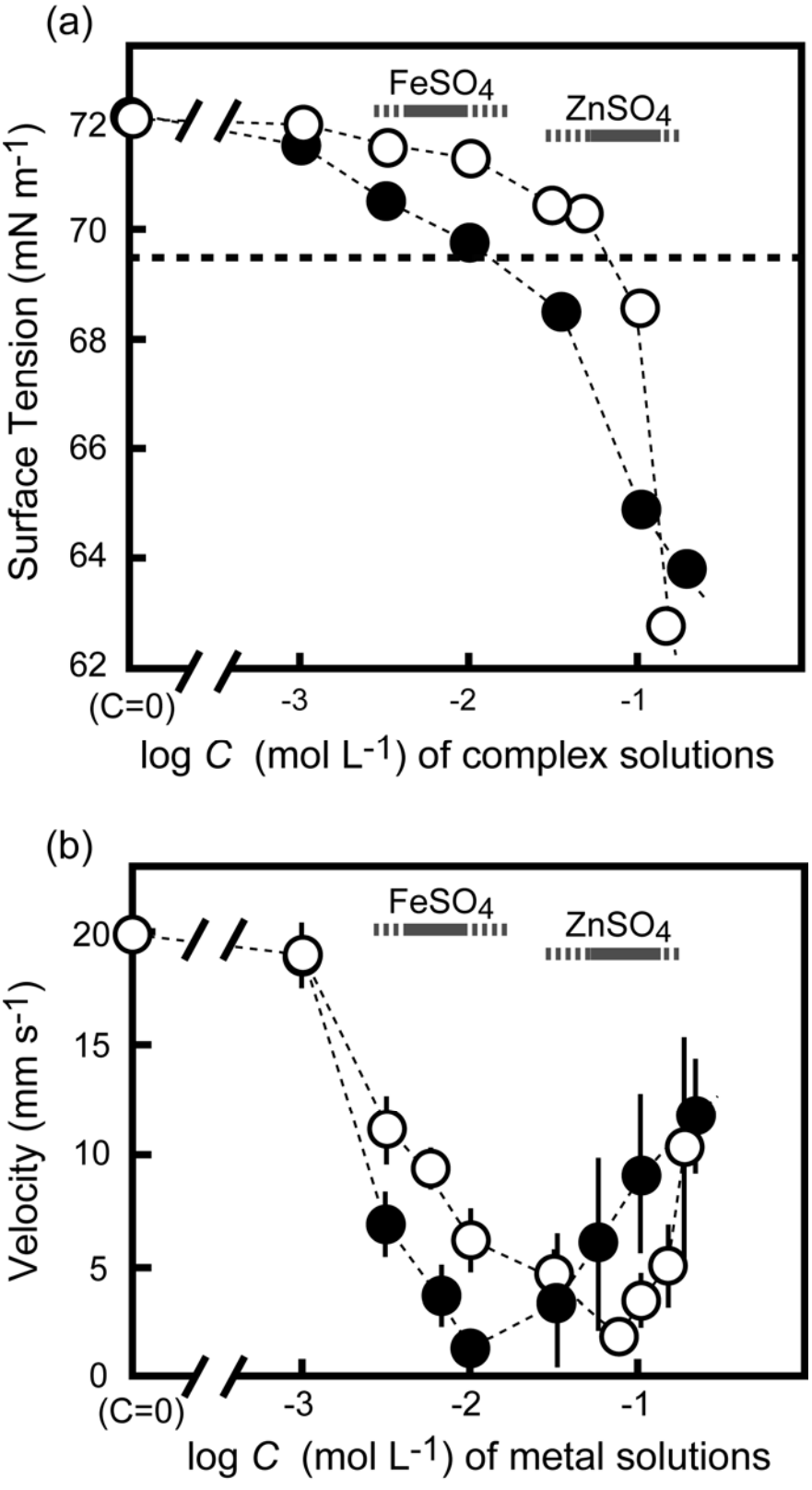
(a)
FeSO4
ZnSO4
Surface Tension (mN m-1)
72
70
68
66
64
62
(C=0)
-3
-2
-1
log C (mol L-1) of complex solutions
(b)
FeSO4
ZnSO4
Velocity (mm s-1)
20
15
10
5
0
(C=0)
-3
-2
-1
log C (mol L-1) of metal solutions

Figure 4

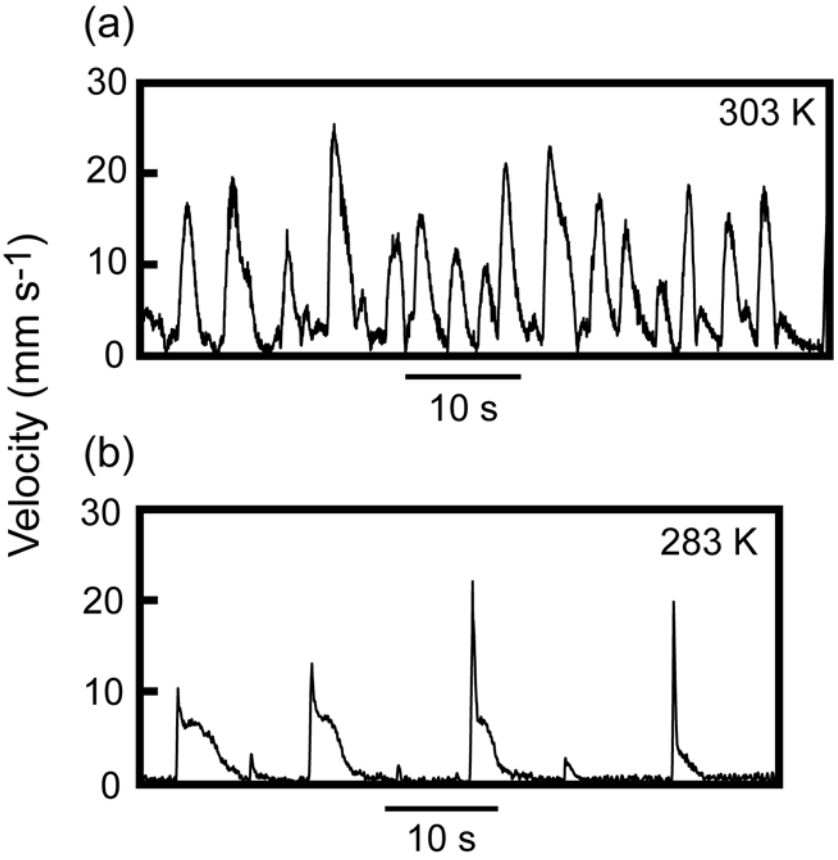

Figure 5

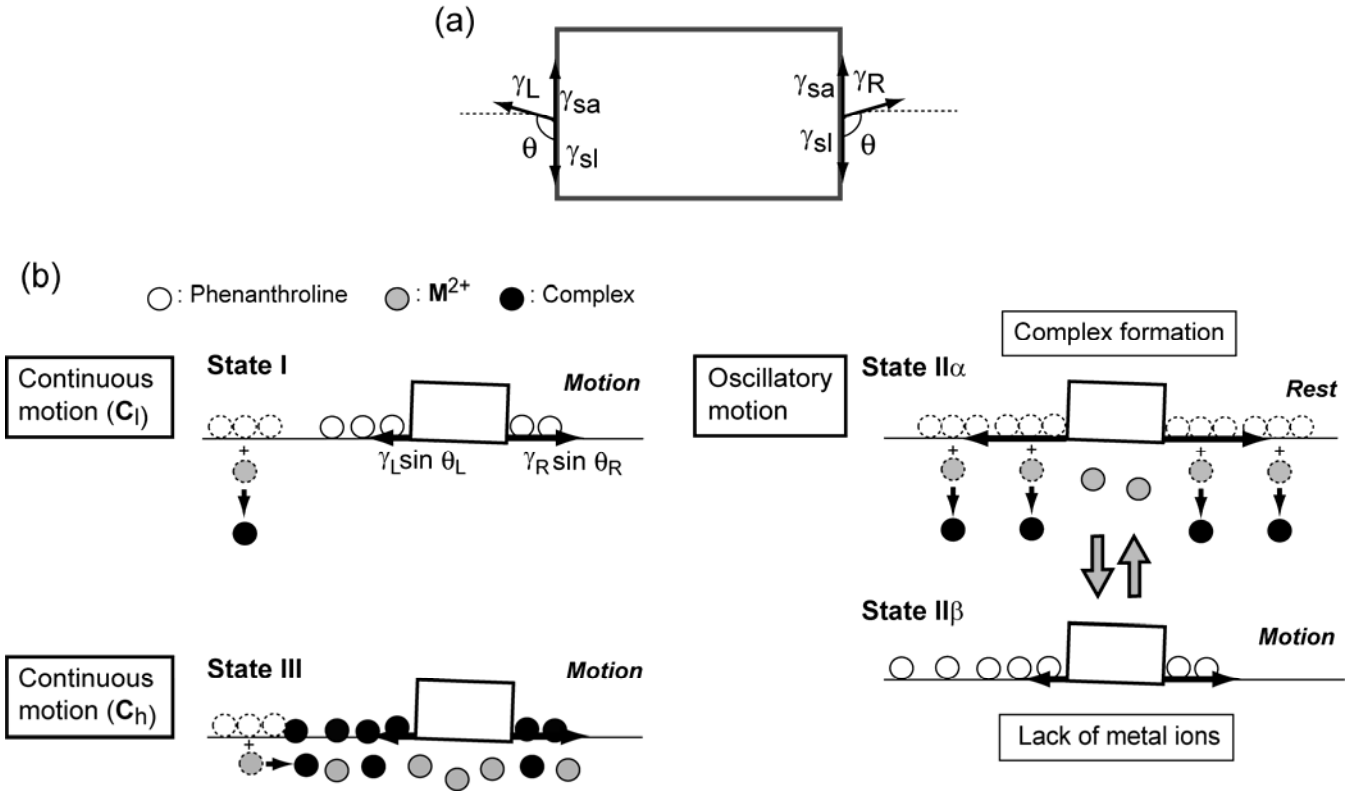
(a)
γL
γsa
θ
γsl
γsa
γR
γsl
θ
(b)
○ : Phenanthroline
● : M2+
● : Complex
Continuous motion (CI)
State I
Motion
γLsin θL
γRsin θR
Continuous motion (Ch)
State III
Motion
Oscillatory motion
Complex formation
State IIα
Rest
State IIβ
Motion
Lack of metal ions

Figure 6

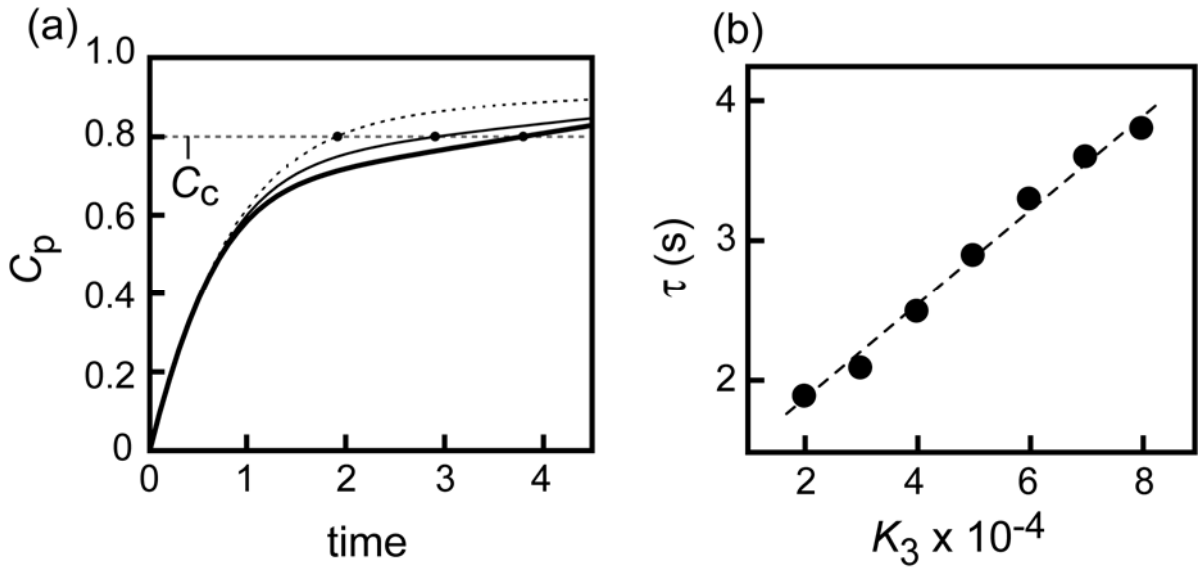

Figure 7